

States of  $^{86}\text{Rb}$ : The  $^{88}\text{Sr}(d, \alpha)^{86}\text{Rb}$  Reaction\*

J. J. Kolata, W. W. Daehnick, and J. E. Holden

*Nuclear Physics Laboratory, University of Pittsburgh, Pittsburgh, Pennsylvania 15213*

(Received 22 May 1972)

The  $^{88}\text{Sr}(d, \alpha)^{86}\text{Rb}$  reaction has been studied with 17.00-MeV deuterons. Energy resolution of 11 keV was obtained using an Enge split-pole spectrograph. Accurate excitation energies ( $\pm 0.15\%$ ) were measured for more than 35 states up to an excitation energy of 3.3 MeV in the residual nucleus. Differential cross sections were obtained for most of the  $^{86}\text{Rb}$  states for  $12.5^\circ \leq \theta \leq 65^\circ$ , and compared with distorted-wave calculations. The deduced  $L$ -transfer values allowed the assignment of a narrow range of  $J^\pi$  values to 25 of these states. Several unique spin assignments were possible. Microscopic-model calculations were performed for several of the low-lying negative parity states in  $^{86}\text{Rb}$ , using simple two-component wave functions empirically derived from  $^{87}\text{Rb}(d, t)$  spectroscopic factors. The predictions agreed reasonably well with the experimental  $(d, \alpha)$  data for both the relative magnitudes and the shapes of the angular distributions, except for the  $J^\pi = 2^-$  ground state.

## I. INTRODUCTION

Recent studies of odd-odd nuclei which are two particles removed from a stable core have shown promise to be of great value in understanding the nucleon-nucleon residual interaction.<sup>1</sup> In each case, it was possible to make detailed comparisons between single-nucleon or two-nucleon transfer data and the predictions of existing shell-model calculations. The  $^{88}\text{Sr}$  nucleus, though it is not doubly magic, may be described in a small enough basis<sup>2</sup> to make shell-model calculations practical for the predominantly two-hole states in  $^{86}\text{Rb}$ . A detailed study of the spectroscopy of  $^{86}\text{Rb}$  would be expected to lead to direct information on the  $f$ - $p$  shell residual interaction.

The  $(d, p)$  and  $(n, \gamma)$  experiments on  $^{86}\text{Rb}$  by Dawson, Sheline, and Journey<sup>3</sup> and three exploratory  $(d, t)$  spectra represent virtually all that was previously known of this nucleus.<sup>4</sup> Current, as yet unpublished work includes investigations of the  $(d, t)$ ,<sup>5</sup>  $(^3\text{He}, \alpha)$ ,<sup>6</sup> and  $(d, ^3\text{He})$ <sup>7</sup> reactions to states in  $^{86}\text{Rb}$ . In the present paper, we present accurate excitation energies and narrow  $J^\pi$  limits (including some unique assignments) for most of the states up to 2.5 MeV in  $^{86}\text{Rb}$ . The low-lying negative-parity states, which are expected to have the least complicated configurations, are discussed in terms of simple two-component shell-model wave functions empirically derived from the  $(d, p)$  and  $(d, t)$  spectroscopic strengths.

## II. EXPERIMENTAL METHOD

The  $^{88}\text{Sr}(d, \alpha)^{86}\text{Rb}$  experiment was performed with a 17.00-MeV deuteron beam from the University of Pittsburgh three-stage Van de Graaff accelerator. This beam was focused through a 0.5-

mm-wide by 2-mm-high collimating slit (followed by an antiscattering slit) placed about 2 cm from the target position in the scattering chamber. The maximum angular divergence of the incident beam was always less than  $\pm 0.5^\circ$ . At the most forward angles ( $\theta \leq 20^\circ$ ), the 0.5-mm collimating aperture was replaced by a 1.0-mm-wide slit to further reduce slit scattering, at some expense in energy resolution. The incident beam was continuously monitored by two NaI(Tl) scintillators at  $\pm 38^\circ$  relative to the beam direction. Deuterons elastically scattered into these counters, as well as the charge collected in a Faraday cup, were used to normalize the relative differential cross sections at the various angles.

The targets were typically  $30\text{-}\mu\text{g}/\text{cm}^2$  films of enriched (99.84%)  $^{88}\text{SrO}$  evaporated onto  $30\text{-}\mu\text{g}/\text{cm}^2$  C backings. Target thickness was determined from three independent measurements. First, Rutherford scattering of 15.00-MeV  $\alpha$  particles was measured with the spectrograph at  $25^\circ$ . Next the targets were bombarded with 11.80-MeV deuterons and the number of particles elastically scattered into the spectrograph at  $\theta_{\text{lab}} = 40^\circ$  was compared with known<sup>8</sup> absolute cross sections for the elastic scattering of 11.8-MeV deuterons from Sr. Finally, the elastic scattering of 17.00-MeV deuterons into the monitor detectors was compared with optical-model predictions using standard parameters.<sup>9</sup> The three methods agreed to within  $\pm 15\%$ , which is the estimated uncertainty in the absolute cross sections.

The reaction  $\alpha$  particles were detected in 50- $\mu\text{m}$  Ilford K-1 nuclear emulsions placed in the focal plane of an Enge split-pole spectrograph. A typical spectrum is shown in Fig. 1. Major contributions to the experimental energy resolution come from beam divergence ( $\approx 8$  keV) and spot size

( $\approx 6$  keV), differential energy loss and straggling in the target ( $\leq 5$  keV), beam energy spread and spectrograph aberrations ( $\leq 3$  keV), and plate-scanning resolution ( $\approx 4$  keV). Taking all the above factors into account, the total experimental energy resolution should be better than 12 keV. The measured full width at half maximum (FWHM) is 11 keV.

Broad groups due to light-element contaminants, which are kinematically defocused by the spectrograph, can also be seen in Fig. 1. These groups obscured peaks of interest at several angles resulting in some gaps in the angular distributions. Only the strongest  $\alpha$  groups were analyzed above an excitation energy of 2.5 MeV because of the rather high density of weak states in this region. Some of these groups were slightly broader than expected from the experimental energy resolution and may in fact correspond to doublets. At the most forward angles ( $\theta \leq 20^\circ$ ), the nuclear emulsions were replaced by an array of position-sensitive counters with which slit-scattering effects could be more easily measured and minimized. A detailed description of this detector array has been given previously.<sup>10</sup> Cross sections could not be obtained at these forward angles for weak levels due to background from pileup of inelastically scattered deuterons, which also determined the most forward angle measured ( $12.5^\circ$ ).

Accurate excitation energies for states observed in this experiment were obtained by direct comparison<sup>11</sup> to states of  $^{58}\text{Co}$  excited in the  $^{60}\text{Ni}(d, \alpha)^{58}\text{Co}$  reaction.<sup>12</sup> The  $^{60}\text{Ni}(d, \alpha)$  and  $^{88}\text{Sr}(d, \alpha)$  reactions were observed on the same photographic plate, with the laboratory angle, incident beam energy (15.00 MeV), spectrograph magnetic-field setting, and focal-plane adjustment held fixed. The dominant contribution to excitation-energy

errors is the rms uncertainty in the  $^{88}\text{Sr}$  peak centroids and the  $^{58}\text{Co}$  standard spectrum energies. We chose to calibrate against the best-known states in  $^{58}\text{Co}$  to reduce this uncertainty as much as possible.

### III. RESULTS AND DISCUSSION

#### A. Assignment of Level Energies

The excitation energies determined in this experiment are listed in Table I. They are believed to be accurate to  $\pm 1.5$  keV or  $\pm 0.15\%$  (whichever is greater). Several of the weaker states listed in Table I have larger assigned errors, reflecting larger rms deviations in excitation-energy measurements at the various angles for which data was taken. Some of the states above 2.5 MeV, in particular the 3.271- and 3.319-MeV levels, probably are unresolved doublets which could have a drastic effect on the measured excitation energy.

Also listed in Table I are the excitation energies for states in  $^{86}\text{Rb}$  from the  $(d, p)$  and  $(n, \gamma)$  experiments<sup>3</sup> and from the  $(d, t)$  data of Ref. 5. Excitation energies for states above 1.5 MeV from  $(n, \gamma)$  were not given in Ref. 3 because of the lack of corroborating evidence. However, we have been able to place 25 of the 28 primary  $\gamma$ -ray transitions to states below 2.5 MeV in  $^{86}\text{Rb}$  within the quoted errors of Ref. 3 and the present study. Of the remaining 11 primary transitions to higher-lying states, only one matched a  $(d, \alpha)$  level. This is not surprising since we have not analyzed the weaker states above 2.5 MeV. The 1.667-MeV state (Table I) was not previously known, but the observed (secondary) 1.668-MeV  $\gamma$  ray is almost certainly the ground-state branch of this level.

In the subsequent discussion, all references to

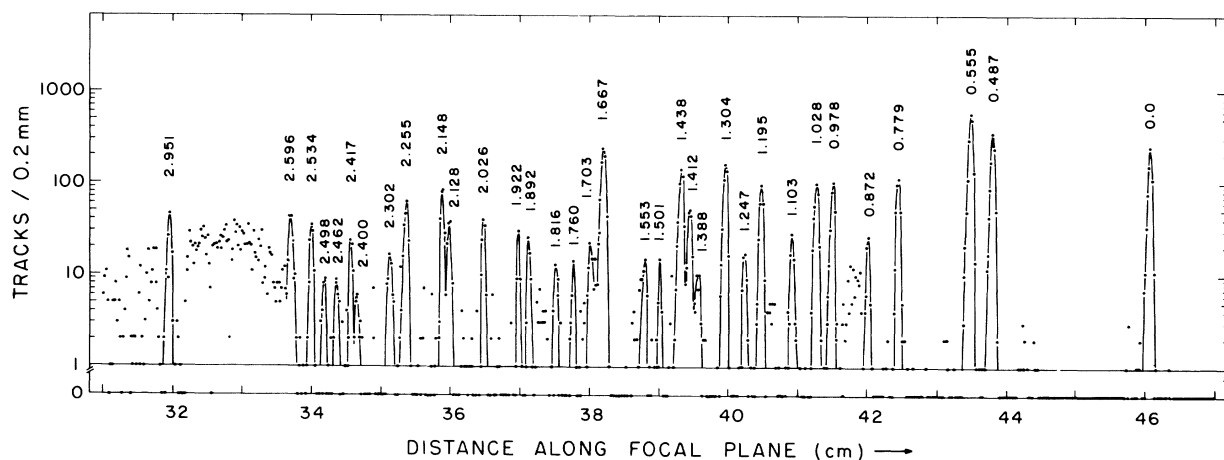


FIG. 1. Typical spectrum for the  $^{88}\text{Sr}(d, \alpha)^{86}\text{Rb}$  reaction, taken at  $\theta_{\text{lab}} = 45^\circ$ . The excitation energies for the  $^{86}\text{Rb}$   $\alpha$  groups are labeled in MeV. The broad groups are due to light-element contaminants.

TABLE I. Experimental excitation energies,  $L$  transfers, and maximum cross sections for  $^{86}\text{Sr}(d, \alpha)^{86}\text{Rb}$ . The notation D after a level indicates that it is a known or suspected doublet. Also listed are excitation energies and  $l$ -transfer values from  $^{87}\text{Rb}(d, t)^{86}\text{Rb}$  (Ref. 5) and  $^{85}\text{Rb}(d, p)^{86}\text{Rb}$  (Ref. 3), along with excitation energies derived from a neutron-capture  $\gamma$ -ray study (Ref. 3). The last two columns list spin and parity limits, and the best  $J^\pi$  deduced from available evidence. Less certain values are enclosed in parentheses.

Level	$E(d, \alpha)$ (MeV)	$E(d, t)$ (MeV)	$E(d, p)$ (MeV)	$E(n, \gamma)$ (MeV)	$\sigma_{\max}(d, \alpha)$ ( $\mu\text{b}/\text{sr}$ )	$L_{d, \alpha}$	$l_{d, t}$	$l_{d, p}$	$J^\pi$ Limits from transfer reactions	Best $J^\pi$
0	0.000	0.000	0.000	0.000	105	1	2+0	4	(0) <sup>-</sup> -2 <sup>-</sup>	2 <sup>-</sup>
1	0.487	0.489	0.486	0.488	175	0+(2)	1	1	1 <sup>+</sup>	1 <sup>+</sup>
2[D]	0.555	0.556	0.556	0.555 0.557	225	3+5	4	4	(2) <sup>-</sup> -6 <sup>-</sup>	(6) <sup>-</sup> + (3) <sup>-</sup>
3[D?]	0.779		0.781	0.779	34	(3)+(7)	?	4	2 <sup>-</sup> -7 <sup>-</sup>	(7) <sup>-</sup>
4	0.872	0.872	0.874	0.873	12	3	4	4	(2) <sup>-</sup> -4 <sup>-</sup>	(3) <sup>-</sup>
5	0.978	0.977	0.981	0.978	49	3	4	4	(2) <sup>-</sup> -4 <sup>-</sup>	(4) <sup>-</sup>
6	1.028	1.027	1.028	1.027	76	2	1	1	1 <sup>+</sup> -3 <sup>+</sup>	(2) <sup>+</sup>
7[D]	1.103	1.091 1.105 1.122 1.156	1.093	1.092 1.106	16	4 or (3+5)	4 3+1 1 1	(4+2)	4 <sup>-</sup> -6 <sup>-</sup> 3 <sup>+</sup> -4 <sup>+</sup> 0 <sup>+</sup> -3 <sup>+</sup> 0 <sup>+</sup> -3 <sup>+</sup>	(5) <sup>-</sup> (3) <sup>+</sup> (0) <sup>+</sup> (4) <sup>-</sup>
8	1.195	1.195	1.197	1.196	55	3+(5)	2+4	4	2 <sup>-</sup> -4 <sup>-</sup>	(4) <sup>-</sup>
9	1.247	1.245	1.251	1.247	6	5	4	(4+2)	4 <sup>-</sup> -6 <sup>-</sup>	(5) <sup>-</sup>
10[D]	1.304	1.304	1.309	1.305 1.309	94	4	1		3 <sup>+</sup> -5 <sup>+</sup>	(3) <sup>+</sup>
11	1.388	1.389	1.390	1.390	9	4	1	1	3 <sup>+</sup> -5 <sup>+</sup>	3 <sup>+</sup>
12	1.412	1.412	...	...	26	5	4		4 <sup>-</sup> -6 <sup>-</sup>	
13	1.438	1.438	1.438	1.439	86	3	(2)		2 <sup>-</sup> -4 <sup>-</sup>	
	...	1.470	1.472	1.470			1	(4+2)	0 <sup>+</sup> -3 <sup>+</sup>	(2) <sup>+</sup>
14	1.501	1.500	1.502	1.501	5	(5, 4)	1	(4+2)	(0 <sup>+</sup> -3 <sup>+</sup> )	
15	(1.553 $\pm$ 4)	1.547	1.554		7	5	4		4 <sup>-</sup> -6 <sup>-</sup>	
16	1.667	1.668	...	1.668	170	2	1		1 <sup>+</sup> -3 <sup>+</sup>	(2) <sup>+</sup>
17	(1.703 $\pm$ 4)	1.708	1.707 1.738	1.708	28	2	1		1 <sup>+</sup> -3 <sup>+</sup>	
18	1.760	1.762			5	(0)	1		1 <sup>+</sup> -3 <sup>+</sup>	(1) <sup>+</sup>
19	(1.816 $\pm$ 4)	...	1.816	1.820	4					
20	1.892	1.892	1.901	1.892	14	2	3+1		1 <sup>+</sup> -3 <sup>+</sup>	
21[D?]	1.922	1.919	1.928	1.916 1.926	17	(3+5)	?			
22	2.026		2.023 2.095		31	4			(3 <sup>+</sup> -5 <sup>+</sup> )	
23	2.128			2.131	28	4			(3 <sup>+</sup> -5 <sup>+</sup> )	
24	2.148			2.148	60	2			(1 <sup>+</sup> -3 <sup>+</sup> )	
	...		2.175	2.180						
25	2.255				15	(6)				
26	(2.270 $\pm$ 3)		2.282	2.266	8	(4, 5)				
	...		2.299	...						
27	2.302		2.337 2.369	2.299 2.332	12	(4)				
28	2.400			2.404	5	(5)				
29	2.417		2.437	...	7	?				
30	2.462			2.462	5	(5)				
31	2.498				3	(4)				
32	2.534				17	2			(1 <sup>+</sup> -3 <sup>+</sup> )	
33	2.596			2.598	18	0			1 <sup>+</sup>	1 <sup>+</sup>
34	2.758				9					
35	2.951				17	0			1 <sup>+</sup>	1 <sup>+</sup>
36	3.271				12					
37	3.319				20					

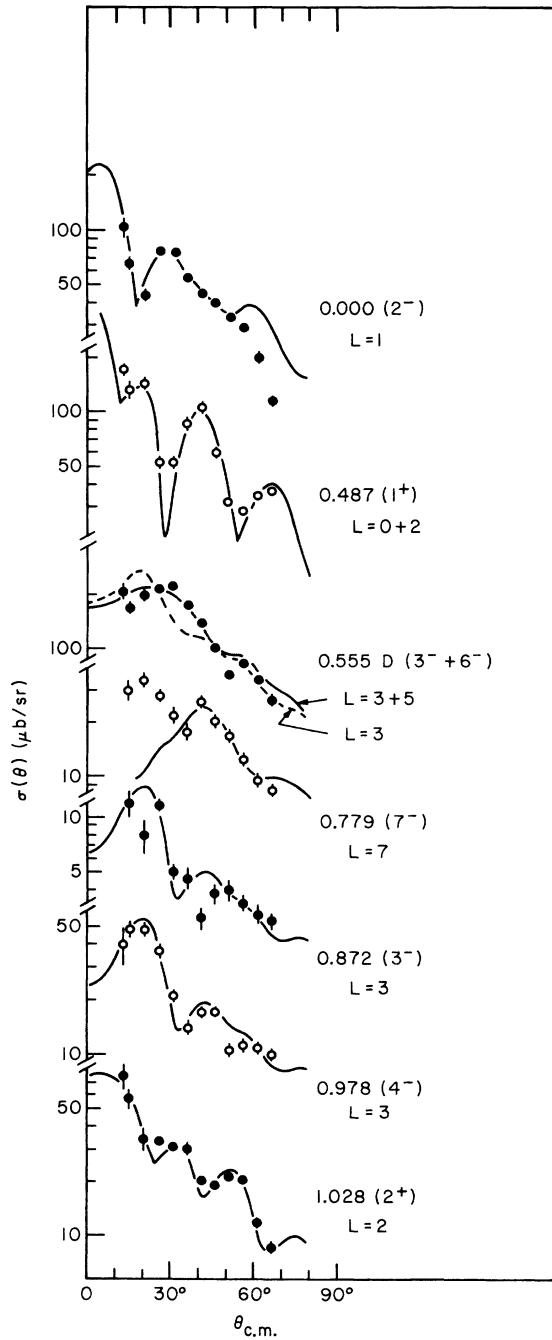


FIG. 2. Angular distributions for  $(d, \alpha)$  transitions to states in the first MeV of excitation in  $^{86}\text{Rb}$ . Excitation energies are given in MeV, and  $L$  transfer and best  $J^\pi$  values are indicated. The notation D indicates a known doublet. The error bars on the data points include statistical errors and an estimate of errors in background subtraction and in the separation of close-lying states. The curves are microscopic DWBA calculations for the negative-parity states (see text), and deuteron cluster calculations for the positive-parity states. All curves are individually normalized to the data.

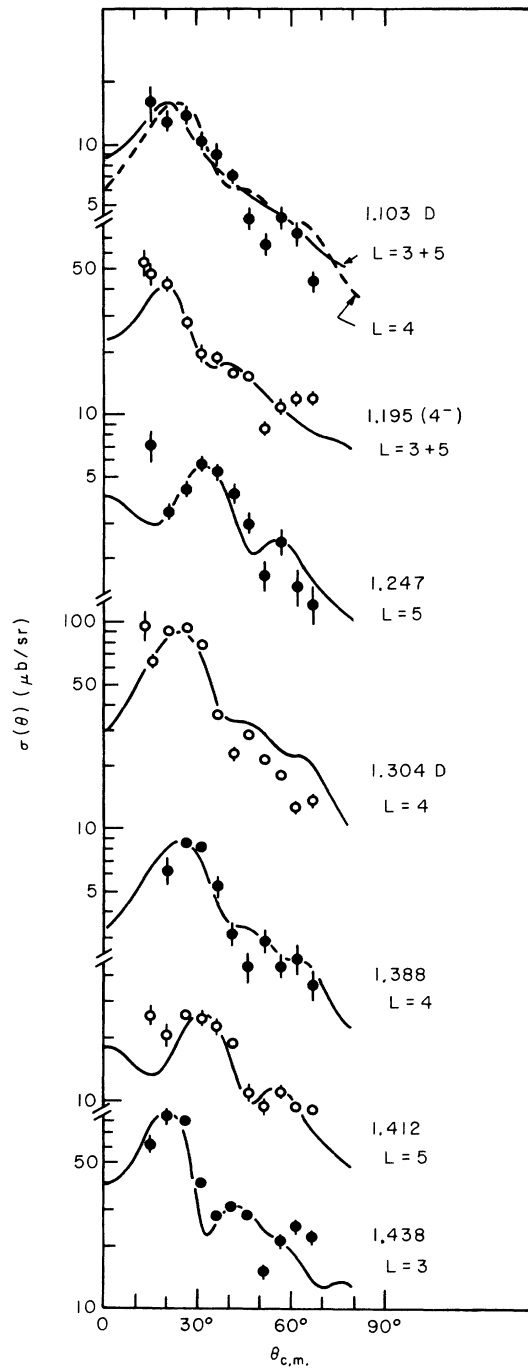


FIG. 3. Angular distributions for transitions to states from 1.0 to 1.5 MeV of excitation in  $^{86}\text{Rb}$ . Excitation energies are given in MeV, and the  $L$  transfer and best  $J^\pi$  values are indicated. The notation D indicates a known doublet. The error bars on the data points include statistical errors and an estimate of errors in background subtraction and in the separation of close-lying states. The curves are DWBA cluster transfer calculations individually normalized to the experimental data.

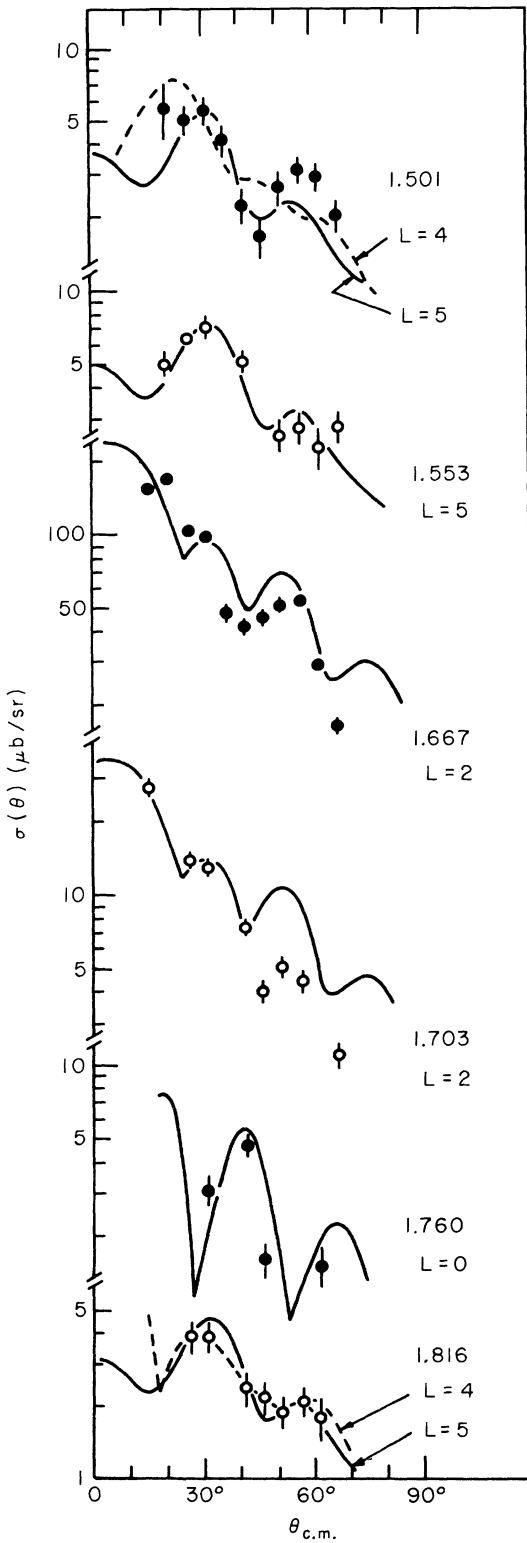


FIG. 4. Angular distributions for transitions to the states between 1.5 and 1.8 MeV of excitation in  $^{86}\text{Rb}$ . See also Fig. 3 caption.

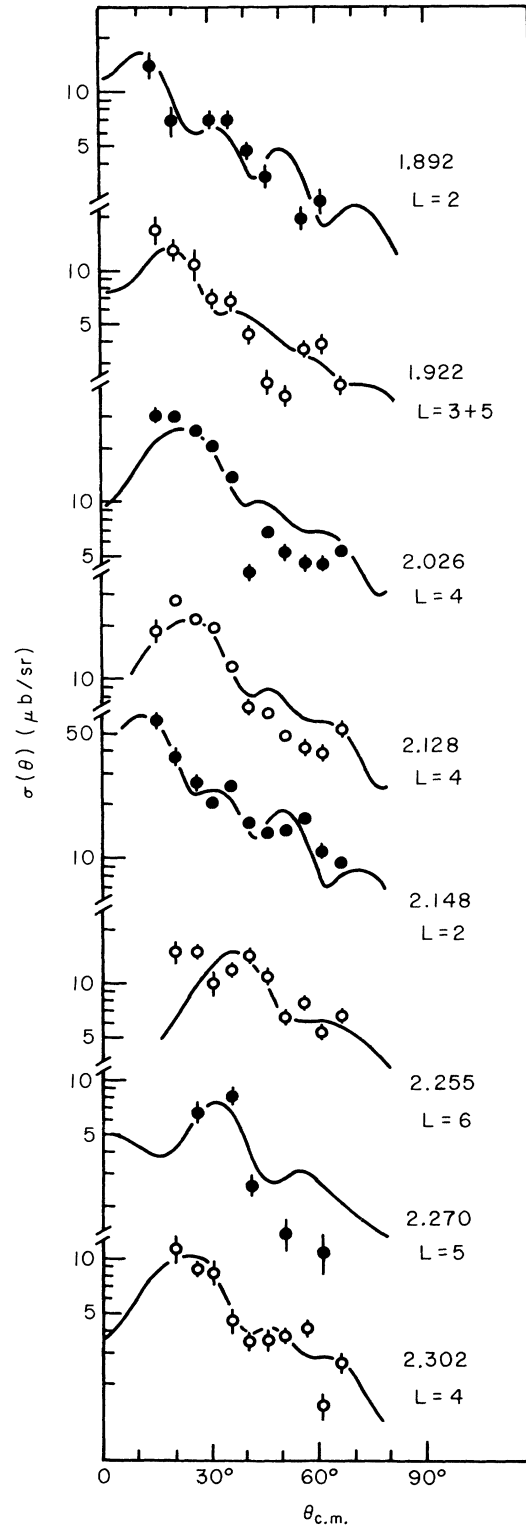


FIG. 5. Angular distributions for transitions to states between 1.8 and 2.3 MeV excitation in  $^{86}\text{Rb}$ . See also Fig. 3 caption.

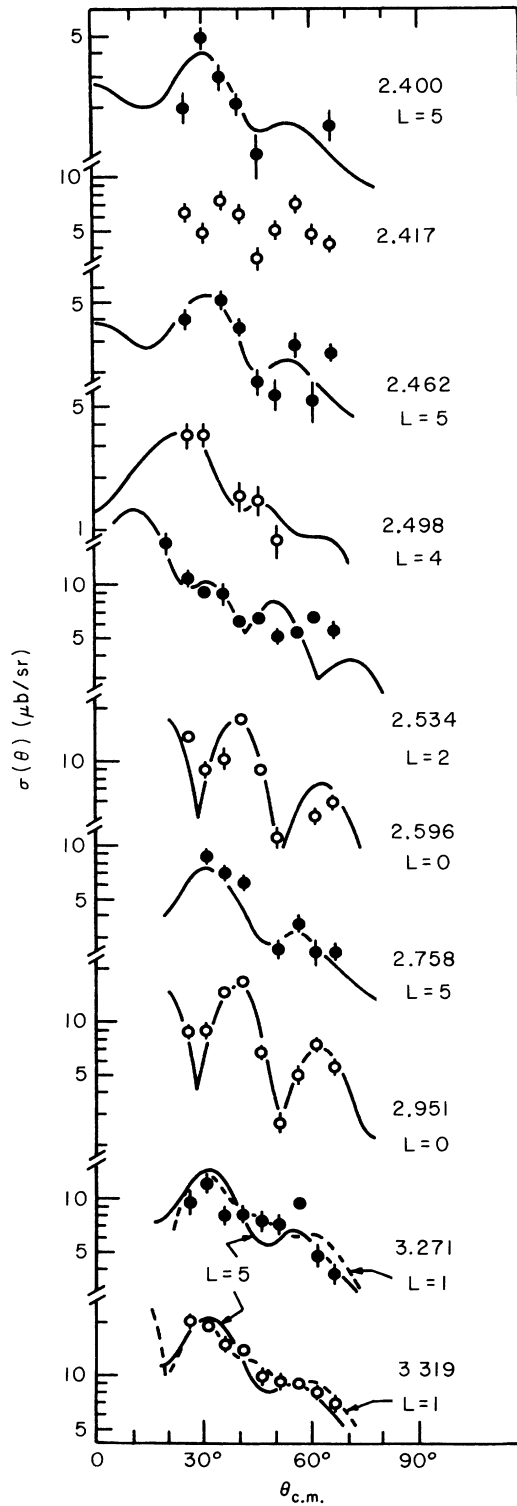


FIG. 6. Angular distributions for transitions to the stronger states in  $^{86}\text{Rb}$  between 2.4 and 3.3 MeV. The two states above 3 MeV are likely to be doublets. See also Fig. 3 caption.

the  $(d, p)$  and  $(n, \gamma)$  data refer to Ref. 3, and those to  $(d, t)$  data refer to Ref. 5.

#### B. Distorted-Wave Analysis

Angular distributions for transitions to all of the states listed in Table I were obtained and are shown in Figs. 2–6. The error bars are primarily due to counting statistics (standard deviation), but include an estimate of errors in background subtraction for weak states and in the separation of partially overlapping close-lying levels. The random monitoring uncertainty of  $\approx 5\%$  was the dominant error for the strongest groups. The experimental angular distributions are compared with predictions of the distorted-wave Born approximation (DWBA) calculated with the code DWUCK.<sup>13</sup> Because of the lack of detailed microscopic wave functions, most of the calculations were made using cluster-model form factors obtained by binding a deuteron in a Woods-Saxon well with parameters given in Table II, at the correct deuteron separation energy. The optical-model parameters used in the calculations are also listed in Table II. Finite-range and nonlocality corrections were computed in the local-energy approximation.<sup>14</sup> The finite-range parameter was 0.4,<sup>15</sup> and the nonlocality parameters were  $\beta_d = 0.54$  and  $\beta_\alpha = 0.2$ .<sup>13</sup> Nonlocal corrections were not applied to the bound-state wave functions. The calculations with finite-range corrections shown in Figs. 2–6 using the parameters of Table II differ only insignificantly from zero-range calculations.

As apparent from Table II, all optical-model and bound-state well parameters were chosen to satisfy the well-matching condition, which has been found essential for  $(d, \alpha)$  transfer calculations.<sup>16</sup> A deviation from this condition leads to much poorer DWBA predictions for  $^{88}\text{Sr}(d, \alpha)^{86}\text{Rb}$ . A deuteron-cluster form factor generated with a well geometry of  $r_0 = 1.20$  fm,  $a = 0.75$  fm corresponds to a microscopic form factor generated with single-nucleon well parameters  $r_0 = 1.25$ ,  $a = 0.65$  fm. Hence these sets of parameters were chosen for cluster and microscopic form factors, respectively. Angular momentum transfer values determined by comparison with DWBA calculations are listed in Table I along with the  $(d, p)$  and  $(d, t)$  assignments. Less certain values are enclosed in parentheses. It should be noted that the  $L$ -value assignments to states above 2.0 MeV are more uncertain since the  $(d, t)$   $l$  values, which reliably determine the parity of the state in question, do not exist. In addition, some of the states above 2.5 MeV, and in particular the 3.271- and 3.319-MeV levels, are likely to be doublets.

The selection rules for the  $(d, \alpha)$  reaction place narrow limits on the spin and parity of a state

whose  $L$ -transfer value is known. These limits are listed in Table I, along with the "best value" for  $J^\pi$  which can be deduced from presently available evidence. The observation of an  $L=0$  transition results in a unique  $J^\pi = 1^+$  assignment.

For some of the low-lying negative-parity states, microscopic-model DWBA calculations were performed with the two-nucleon-transfer version of DWUCK, which uses the method of Bayman and Kallio.<sup>17</sup> The appropriate bound-state parameters are listed in Table II. The separation energies of the single nucleons were each taken to be equal to one-half the deuteron-separation energy plus the excitation energy of the  $^{86}\text{Rb}$  level. An  $\alpha$ -particle rms radius of 1.4 fm was used in the calculations.<sup>18</sup>

The wave functions for the lowest negative-parity states (Table III) were taken as simple two-component configurations of the form

$$\psi_J = \alpha_J | \pi p_{3/2}^{-1} \nu g_{9/2}^{-1} \rangle_J + \beta_J | \pi f_{5/2}^{-1} \nu g_{9/2}^{-1} \rangle_J,$$

with an inert  $^{88}\text{Sr}$  core. The  $l=4$  spectroscopic factor for the  $(d, t)$  reaction on the  $p_{3/2}$  ground state of  $^{87}\text{Rb}$  (assumed to be pure proton hole) to the state  $\psi_J$  is a measure of the  $\alpha_J$  coefficient, and  $\beta_J$  is obtained from the normalization  $\alpha_J^2 + \beta_J^2 = 1$ . The expected  $(d, p)$  spectroscopic strength is then computed under the assumption that the  $^{85}\text{Rb}$  ground state is a pure  $(\pi f_{5/2}^{-1}, \nu g_{9/2}^{-2})$  configuration and that all the  $l=4$  strength comes from the filling of one of the  $g_{9/2}$  neutron holes. These calculated  $(d, p)$  strengths (Table III) are in good agreement with experiment for six of the seven lowest-lying negative-parity states, the exception being the  $J^\pi = 2^-$  ground state which has about twice the predicted strength. The negative-parity states above 1.2 MeV require  $\geq 50\%$  admixtures of additional configurations to account for both the  $(d, p)$  and  $(d, t)$  spectroscopic strengths. Microscopic-model calculations were not made for these states, nor for the positive-parity states which require multicomponent wave functions even in the first-order shell-model approach.

### C. Low-Lying States in $^{86}\text{Rb}$

$E_x = 0.000 \text{ MeV}$ . All experimental evidence is consistent with the  $J^\pi = 2^-$  assignment based on atomic-beam measurements<sup>19</sup> and the  $(d, p)$  experiment. The first-order shell model based on a closed  $^{88}\text{Sr}$  core requires a pure  $(\pi f_{5/2}^{-1}, \nu g_{9/2}^{-1})$  configuration which is not in agreement with the measured  $(d, p)$  spectroscopic strength, as mentioned above, nor with the fact that the state is seen in  $(d, t)$  with  $l=0+2$ . The microscopic-model prediction for this configuration (Fig. 2) is dominated by  $L=1$  as observed, but the predicted cross section (Table IV), normalized to the presumably pure  $7^-$  member of this multiplet, is about a factor of 4 too small.

$E_x = 0.487 \text{ MeV}$ . The characteristic  $L=0$  angular distribution for the transition to this state (Fig. 2) serves to uniquely assign  $J^\pi = 1^+$ . The  $LS$ - $JJ$  transformation coefficients for  $(\pi p_{3/2}^{-1}, \nu p_{1/2}^{-1})$  and  $(\pi p_{3/2}^{-1}, \nu p_{3/2}^{-1})$  configurations predict a predominantly  $L=0$  angular distribution as observed. The remaining first-order transfers that could contribute to this state are dominated by  $L=2$ .

$E_x = 0.555 \text{ MeV}$ . This state is a known doublet and all experimental evidence is consistent with  $6^-$  and  $3^-$  assignments to the two components. The microscopic-model prediction for the cross section summed over both states (solid curve) is in excellent agreement with the observed  $L=(3+5)$  mixture. A similar calculation made for a pure  $(\pi f_{5/2}^{-1}, \nu g_{9/2}^{-1})$  configuration for both states (dashed curve) predicts a nearly pure  $L=3$  angular distribution. The predicted cross section (Table IV) summed over both states, is a factor of 1.4 smaller than observed.

$E_x = 0.779 \text{ MeV}$ . This state has negative parity and its decay is consistent with a  $J^\pi = 7^-$  assignment. It is very weakly populated in the  $(d, t)$  reaction, which is to be expected for the  $7^-$  member of the  $(\pi f_{5/2}^{-1}, \nu g_{9/2}^{-1})$  multiplet. The  $(d, \alpha)$  angular distribution (Fig. 2) is consistent with  $L=7$  above  $25^\circ$ , but not in the forward direction. This

TABLE II. Optical-model parameters used in the  $^{88}\text{Sr}(d, \alpha)^{86}\text{Rb}$  distorted-wave calculations. These are the "well-matched" parameters of Ref. 16. Also listed are the bound-state well parameters for a deuteron cluster and for individual nucleons (microscopic-model calculation).

	$V$ (MeV)	$r_0$ (fm)	$r_c$ (fm)	$a$ (fm)	$W$ (MeV)	$W_D$ (MeV)	$r_I$ (fm)	$a_I$ (fm)	$\lambda_{50}$
Incident channel ( $d + ^{88}\text{Sr}$ )	90.0	1.20	1.30	0.75	0	16.6	1.30	0.70	
Exit channel ( $\alpha + ^{86}\text{Rb}$ )	181.3	1.20	1.30	0.75	15.0	0	1.70	0.60	
Bound deuteron	a	1.20	1.30	0.75					0
Bound nucleons	a	1.25	1.30	0.65					25.0

<sup>a</sup> Well depth adjusted to give the proper separation energy.

state is strong enough and the deviation from the predicted angular distribution is large enough to suggest a possible doublet, with the second component probably displaying an  $L = 3$  angular distribution. This conjecture is supported by the possible feeding of this state from the 1.305-MeV level (probably  $J^\pi = 3^+$ ). This  $\gamma$  line was previously interpreted as merely a coincidental energy balance.<sup>3</sup> The microscopic-model calculations are normalized to this  $(7)^-$  state (Table IV) after subtracting out the assumed  $L = 3$  component.

$E_x = 0.872$  and  $0.978$  MeV. Both states display  $L = 3$  angular distributions in the  $(d, \alpha)$  reaction and  $l = 4$  shapes in the  $(d, t)$  reaction, which limit spin and parity to  $J^\pi = (3, 4)^-$ . The  $\gamma$ -ray decay scheme suggests  $3^-$  for the 0.872-MeV level and  $4^-$  for the 0.978-MeV state. The microscopic-model calculation for the  $3^-$  state leads to good agreement with experiment under the assumption that this state is orthogonal to the first  $3^-$  state at 0.555 MeV (Table III) in our simple two-component model space. Destructive interference between the two components reduces the predicted cross section by nearly a factor of 5 compared to that for the first (enhanced)  $3^-$  state. The angular distribution (Fig. 2) and magnitude of the cross section (Table IV) for the 0.978-MeV  $4^-$  state are reproduced quite well by the microscopic-model calculation. A calculation for a pure  $(\pi f_{5/2}^{-1}, \nu g_{9/2}^{-1})$  configuration would predict a nearly pure  $L = 5$  angular distribution in disagreement with experiment.

$E_x = 1.028$  MeV. The  $L = 2$  angular distribution for this state limits the possible spin and parity assignments to  $J^\pi = (1 - 3)^+$ , which are the same as the limits imposed by the combined  $(d, p)$  and  $(d, t)$   $l$  value assignments. The  $\gamma$ -ray decay of this level suggests  $J^\pi = (1, 2)^+$ . Of these two possibilities,  $J^\pi = 2^+$  seems the most likely. The  $l = 1$  assignment in  $(d, t)$  implies a significant admixture of  $(\pi p_{3/2}^{-1}, \nu p_{3/2}^{-1})$  or  $(\pi p_{3/2}^{-1}, \nu p_{1/2}^{-1})$  configurations which would kinematically favor  $L = 0$  in the

$(d, \alpha)$  angular distribution for a  $1^+$  state, contrary to experiment.

$E_x = 1.103$  MeV. This state is a known doublet and the lower component has odd parity with  $J^\pi = (3 - 6)^-$  as deduced from the  $(d, t)$  reaction. The  $(d, t)$  spectroscopic strength and the  $\gamma$ -ray decay scheme indicate that this component has  $J^\pi = 5^-$ . The  $(d, t)$  data for the upper component require  $J^\pi = (1 - 3)^+$ , with the  $3^+$  assignment favored by the  $\gamma$ -ray decay. Unfortunately, this doublet is not resolved in the  $(d, \alpha)$  experiment. The measured excitation energy (Table I) suggests that mainly the upper component (positive parity) is populated. The angular distribution can be fitted by  $L = (3 + 5)$  as in Fig. 3, or by  $L = 4$ . The upper limit to the  $L = 5$  peak cross section is not in conflict with the  $10 \mu\text{b/sr}$  predicted by the microscopic-model calculation for the  $J^\pi = 5^-$  level.

$E_x = 1.195$  MeV. The  $(d, \alpha)$  angular distribution for this state (Fig. 3) is mainly  $L = 3$  but with a probable  $L = 5$  admixture. This suggests a  $J^\pi = 4^-$  assignment which is consistent with the  $\gamma$ -ray decay of this state.

$E_x = 1.247$  MeV. This transition displays an  $L = 5$  angular distribution, limiting  $J^\pi$  to  $(4, 5, 6)^-$ . The observed  $l = 2$  admixture in  $(d, p)$  eliminates the  $J = 6$  possibility. The decay of this state suggests  $J^\pi = 5^-$ .

$E_x = 1.304$  and  $1.388$  MeV. The  $(d, \alpha)$  and  $(d, t)$  data for these states yield unique  $J^\pi = 3^+$  assignments if only one level is involved. The  $(d, p)$  angular distribution and excitation energy for the 1.304-MeV level led to the suggestion of another (unresolved) state at 1.309 MeV. A weak 530-keV  $\gamma$  ray was then interpreted as the decay of this state to the 0.779-MeV  $7^-$  level, suggesting a  $J^\pi = 6^-$  assignment. The evidence for the existence of the 1.309-MeV level is weak, but it is partially supported by the  $(d, t)$  data. If it does exist, the  $J^\pi = 3^+$  assignment to the 1.304-MeV level is not unique.

$E_x = 1.412$  and  $1.553$  MeV. Transitions to these

TABLE III. Two-component wave functions for the lowest-lying negative-parity states in  $^{86}\text{Rb}$ , empirically derived from the  $^{87}\text{Rb}(d, t)^{86}\text{Rb}$  spectroscopic factor. The last column lists the ratio of experimental to predicted spectroscopic factors obtained for the  $^{85}\text{Rb}(d, p)^{86}\text{Rb}$  reaction using these wave functions, under the assumptions discussed in the text.

$E_x$	$J^\pi$	$\alpha(\pi p_{3/2}^{-1}, \nu g_{9/2}^{-1})_{J^\pi}$	$\beta(\pi f_{5/2}^{-1}, \nu g_{9/2}^{-1})_{J^\pi}$	$\frac{S_{\text{exp}}}{S_{\text{predicted}}}(d, p)$
0.000	$2^-$	0.0	1.0	2.0
0.555	$3^-$	0.68	0.74	
0.555	$6^-$	0.96	0.24	1.1
0.779	$7^-$	0.0	1.0	1.0 <sup>a</sup>
0.872	$3^-$	0.74	-0.68	0.8
0.978	$4^-$	0.92	0.39	1.2
1.091	$5^-$	0.88	0.48	(1.0)

<sup>a</sup> Experimental and predicted spectroscopic strengths normalized to this state.

states display  $L = 5$  angular distributions (Fig. 3) so that  $J^\pi$  is limited to  $(4 - 6)^-$ . The lack of a primary  $(n, \gamma)$  transition to the 1.553-MeV state despite strong  $(d, p)$  population may indicate  $J^\pi = (5, 6)^-$ . On the other hand, it may only be a reflection of the intensity fluctuations expected from a Porter-Thomas distribution.<sup>20</sup>

$E_x = 1.667$  MeV. The  $(d, \alpha)$  and  $(d, t)$  angular distributions for transitions to this state lead to  $J^\pi = (1 - 3)^+$  limits. An unassigned 1667.9-keV transition in the  $(n, \gamma)$  spectrum very probably is the ground-state decay of this level. Unassigned neutron-capture  $\gamma$  rays at 1177.8, 514.8, 165.7, and 120.3 keV fit into the decay scheme for this level as transitions to the 0.487-, 1.156-, 1.501-, and 1.547-MeV states. Since the 1.156-MeV state is probably  $J^\pi = 0^+$  (see below) and the 1.547-MeV state is  $J^\pi = (4, 5, 6)^-$ , the most likely assignment for the spin and parity of the 1.667-MeV state is  $J^\pi = 2^+$ . This suggestion is consistent with the observation that strong  $(d, t)$  population with an  $l = 1$  angular distribution implies admixtures of  $(\pi p_{3/2}^{-1}, \nu p_{3/2}^{-1})$  or  $(\pi p_{3/2}^{-1}, \nu p_{1/2}^{-1})$  which should lead to significant  $L = 0$  strength for a  $1^+$  state, contrary to experiment. One difficulty with this chain of reasoning is the fact that energy differences for transitions from this state to seven other levels below 1.5 MeV are within 3 keV of already-assigned neutron-capture  $\gamma$  rays. While none of these possible transitions is inconsistent with a  $J^\pi = 2^+$  assignment, this result certainly casts doubt on the usefulness of energy balance in the absence of coincidence measurements. The fact that the 1.667-MeV state is not populated by a primary  $(n, \gamma)$  transition does not contribute any new information about its probable spin since the  $(d, p)$  transition is also absent. The most likely explanation is that this state has very little overlap with states constructed from a  $1f_{5/2}$  proton hole.

TABLE IV. Ratio of experimental to predicted  $^{88}\text{Sr}(d, \alpha)^{86}\text{Rb}$  cross sections obtained from microscopic distorted-wave calculations using two-configuration model wave functions listed in Table III.

$E_x$	$J^\pi$	$\sigma_{\text{exp}}^{\text{max}} / \sigma_{\text{predicted}}^{\text{max}}(d, \alpha)$
0.000	$2^-$	3.5
0.555	$3^- + 6^-$	1.4
0.779	$7^-$	1.0 <sup>a</sup>
0.872	$3^-$	0.8
0.978	$4^-$	1.2
1.091	$5^-$	(0.7)

<sup>a</sup> Experimental and predicted cross sections normalized to this state.

#### D. Other States of Interest in $^{86}\text{Rb}$

Two strong  $l = 1$  transitions to states at 1.156 and 1.470 MeV are seen in the  $(d, t)$  reaction, but the corresponding  $(d, \alpha)$  transitions are not observed at all. These data could suggest  $J^\pi = 0^+$  for both states since  $0^+ - 0^+$  transitions are totally forbidden in  $(d, \alpha)$ . However, the 1.470-MeV state is populated by a primary  $\gamma$ -ray transition which is not expected for a  $0^+$  state. In addition, it is observed to decay to both the 1.304-MeV  $(3)^+$  state and the 0.557-MeV  $3^-$  state. All these observations are explained by assuming a  $(p_{3/2}^{-2})_2^+$  configuration for the 1.470-MeV level. In this case, the  $(d, \alpha)$  transition would be inhibited by a somewhat weaker selection rule (based on isospin conservation) forbidding  $(j^2)_{j=\text{even}}$  pickup in  $(d, \alpha)$ .<sup>21</sup> The experimental evidence for the 1.156-MeV state is consistent with a  $J^\pi = 0^+$  assignment for this state.

Four  $L = 0$   $(d, \alpha)$  transitions are observed to states at 0.487, 1.760, 2.596, and 2.951 MeV, resulting in unique  $J^\pi = 1^+$  assignments. The first-order shell model predicts five  $1^+$  states, only two of which are expected to have strong  $L = 0$  components in the absence of configuration mixing because only two are based on  $(p^{-2})$  shell-model states.

The states at 2.026, 2.128, and 2.302 MeV display typical  $L = 4$  angular distributions in  $(d, \alpha)$  resulting in  $J^\pi = (3, 4, 5)^+$  limits. The 2.128- and 2.302-MeV states are populated by primary  $(n, \gamma)$  transitions suggesting  $J^\pi = 3^+$  or perhaps  $4^+$ . The angular distribution for the transition to the state at 2.255 MeV is fitted reasonably well by an  $L = 6$  distorted-wave calculation (Fig. 5), with a possible small admixture of  $L = 4$ . The  $LS$ - $JJ$  transformation coefficients for the  $(f_{5/2}^{-2})_5^+$  state predict a transition dominated by  $L = 6$ .

Finally, it should be noted that there are six states above 2 MeV which are very strongly populated in  $(d, p)$  but are not seen in  $(d, \alpha)$ . These are most probably the one-particle-three-hole states formed by stripping neutrons into orbits above the  $N = 50$  closed shell. Some of these states (i.e., the lower-spin states) are also populated by primary  $(n, \gamma)$  transitions.

#### IV. SUMMARY AND CONCLUSIONS

Accurate excitation energies have been obtained for more than 35 states of  $^{86}\text{Rb}$  populated in the  $^{88}\text{Sr}(d, \alpha)^{86}\text{Rb}$  reaction. Differential cross sections were obtained from 12.5 to 65° laboratory angle, and compared to deuteron-pickup DWBA calculations. The resulting  $L$ -transfer values, along with information from the  $(d, p)$ ,  $(d, t)$ , and neutron-capture reactions to the same final nucleus,<sup>3,5</sup> al-

lowed the assignment of a narrow range of  $J^\pi$  values for 25 of these states. In several cases, it was possible to make unique spin-parity assignments.

Microscopic calculations for the low-lying negative-parity states of  $^{86}\text{Rb}$ , using simple two-component wave functions empirically derived from the  $(d, t)$  spectroscopic factors, have been shown to be reasonably successful in accounting for both the relative magnitudes and angular distributions of  $(d, \alpha)$  transitions to these states. The major discrepancy was the  $L = 1$  transition to the  $J^\pi = 2^-$  ground state, which was about 4 times stronger than expected. Our model wave function for the ground state was also unsuccessful in predicting the  $(d, p)$  spectroscopic factor. It is interesting to note, however, that the enhancement of  $(d, \alpha)$  transitions to the lowest-lying states of spin-parity  $3^- - 6^-$ , and the strongly destructive interference for the second  $3^-$  state at 0.872 MeV in the same reaction, are reproduced by these simple model wave functions. Microscopic-model calculations were not performed for the positive-parity

states, which are expected to be far more complex since they require multicomponent wave functions even in the simplest first-order shell model. Nevertheless, at times it was possible to suggest dominant configurations for positive-parity states from the  $LS$ - $JJ$  transformation coefficients for the appropriate shell-model orbitals.

The success of simple, empirical shell-model wave functions in predicting the negative-parity states in  $^{86}\text{Rb}$  suggests that a sophisticated calculation might be able to account for all the low-lying states in this nucleus. It would certainly be of interest to compare the results of such a calculation with the experimental  $(d, \alpha)$ ,  $(d, t)$ , and  $(d, p)$  reaction data, particularly for the positive-parity states which are at present not well understood.

#### ACKNOWLEDGMENTS

It is a pleasure to acknowledge the fine work of A. Trent and others of the Pittsburgh plate-scanning group.

\*Work supported by the National Science Foundation.

<sup>1</sup>For a general discussion of empirical matrix elements see J. P. Schiffer, in *The Two-Body Force in Nuclei*, edited by S. M. Austin and G. M. Crawley (Plenum, New York, 1972), pp. 205-227. Detailed shell-model calculations are used in: M. B. Lewis and W. W. Daehnick, *Phys. Rev. C* **1**, 1577 (1970); T. S. Bhatia, W. W. Daehnick, and T. R. Canada, *ibid.* **3**, 1361 (1971); M. J. Schneider and W. W. Daehnick, *ibid.* **4**, 1649 (1971); J. J. Kolata and W. W. Daehnick, *ibid.* **5**, 568 (1972).

<sup>2</sup>J. F. Harrison and J. C. Heibert, *Nucl. Phys.* **A185**, 385 (1972).

<sup>3</sup>J. W. Dawson, R. K. Sheline, and E. T. Jurney, *Phys. Rev.* **181**, 1618 (1969).

<sup>4</sup>R. L. Auble, *Nucl. Data* **B5**(No. 2), 151 (1971).

<sup>5</sup>J. E. Holden, J. J. Kolata, and W. W. Daehnick, preceding paper, *Phys. Rev. C* **6**, 1305 (1972).

<sup>6</sup>C. M. Fou, private communication.

<sup>7</sup>M. Noble *et al.*, *Bull. Am. Phys. Soc.* **17**, 72 (1972).

<sup>8</sup>G. Mairle and U. Schmidt-Rohr, Max Planck Institut für Kernphysik (Heidelberg) Report No. 1965 IV 113 (unpublished).

<sup>9</sup>C. M. Perey and F. G. Perey, *Phys. Rev.* **132**, 755 (1963).

<sup>10</sup>W. W. Daehnick, *Phys. Rev.* **177**, 1763 (1969).

<sup>11</sup>We are indebted to J. Childs for the use of his calibration code SPIRO (unpublished).

<sup>12</sup>M. J. Scheider and W. W. Daehnick, *Phys. Rev. C* **5**, 1330 (1972).

<sup>13</sup>FORTTRAN-IV computer code DWUCK and instructions written by P. D. Kunz, University of Colorado (unpublished).

<sup>14</sup>F. G. Perey and D. Saxon, *Phys. Letters* **10**, 107 (1964).

<sup>15</sup>This corresponds to an interaction range of 0.8 fm.

<sup>16</sup>R. DelVecchio and W. W. Daehnick, *Phys. Rev.* (to be published).

<sup>17</sup>B. F. Bayman and A. Kallio, *Phys. Rev.* **156**, 1121 (1967).

<sup>18</sup>H. Frank, D. Haas, and H. Prange, *Phys. Letters* **19**, 391 (1965).

<sup>19</sup>N. Braslau, G. O. Brink, and J. M. Kahn, *Phys. Rev.* **123**, 1801 (1961).

<sup>20</sup>C. E. Porter and R. G. Thomas, *Phys. Rev.* **104**, 483 (1956).

<sup>21</sup>N. K. Glendenning, *Phys. Rev.* **137**, B102 (1965).